Electronic Supplementary Material (ESI) for ChemComm.

Supporting Information for

Sulfur Nanocomposites as Positive Electrode Materials for Rechargeable Potassium-sulfur Batteries

Yu Liu, Weigang Wang, Jing Wang, Yi Zhang, Yusong Zhu, Yuhui Chen, Lijun Fu,*

Yuping Wu*

College of Energy Science and Engineering, Institute of Advanced Materials, Nanjing Tech University, Nanjing 211800, Jiangsu Province, China

Experimental

Synthesis: pyrolyzed polyacrylonitrile/sulfur composite (SPAN) was prepared through a modified process of a previous report.[1] Sulfur was purchased from the Aladdin (Shanghai, China). Polyacrylonitrile (PAN) was purchased from the Aldrich. First, sulfur and polyacrylonitrile in a mass ratio of 4:1 were manually ground to a uniform color and then transferred to a crucible. The mixture was preheated at 155℃ for 1 h and 450℃ for 5 h in Ar with a heating rate of 5℃ min^{-1}. The obtained sample is denoted as SPAN. Carbonized PAN was also prepared by going through a similar heat treatment aforementioned and denoted as CPAN.

Material Characterization: XRD measurements were performed by using a Rigaku D/max-RB instrument using Cu Kα radiation (λ = 1.5418 Å) at a range of 10−90°. Brurauer Emmerr Teller (BET) surface area was measured using a Tristar II3020 instrument by adsorption of nitrogen at 77 K. The content of sulfur is detected by ICP test. The detailed morphology and microstructure of the as-prepared materials were determined by FE-SEM (JEOL, JSM-7100F). XPS (Kratos AXIS Ultra DLD) was applied to study the change of valence state of elements in SPAN. The Raman spectra were collected using an alpha 300 M+ Raman Microscope. Fourier-transform infrared (FTIR) spectra were recorded on a Nicolet Nexus 670 Fourier transform infrared spectrometer (FT-IR) with the KBr pellets method. For characterization of the samples after cycling, they were protected in Argon atmosphere except a short air exposure during the transfer process for the XPS measurement.

Electrochemical Measurements: Coin cells were assembled in a glove box containing pure argon gas. The working electrodes consisted of 80% SPAN active material, 10% acetylene black as conductive agent and 10% polyvinylidene fluoride (PVDF) as binder (using N-methyl-2-pyrrolidone as solvent). In the electrode, the weight of SPAN is ~1 mg cm^{-2}. Potassium discs were used as both the counter and reference electrodes, 0.8 M KPF_6 in a mixture of ethylene carbon (EC)-diethyl carbonate (DEC) (1:1 v/v) was used as the electrolyte. Glass fibre (GF/D) from Whatman was used as separator. Galvanostatic and rate charge - discharge tests were

performed in a potential range of 0.8 - 2.9 V vs. K^+/K using a multichannel battery testing system (LAND CT2001A, P. R. China). Cyclic voltammetry (CV) was recorded on a CHI 660C at a scanning rate of 0.1 mV s^{-1} within the same potential range. The AC impedance spectra were analyzed using a CHI 660C from 100 kHz to 0.001 Hz.

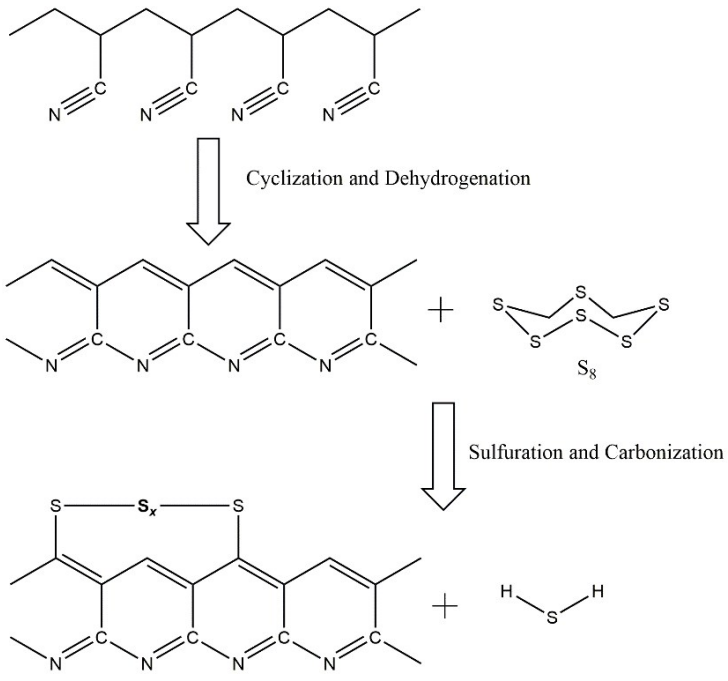

Figure S1. Schematic synthetic process of SPAN ($0 \leqslant x \leqslant 6$).

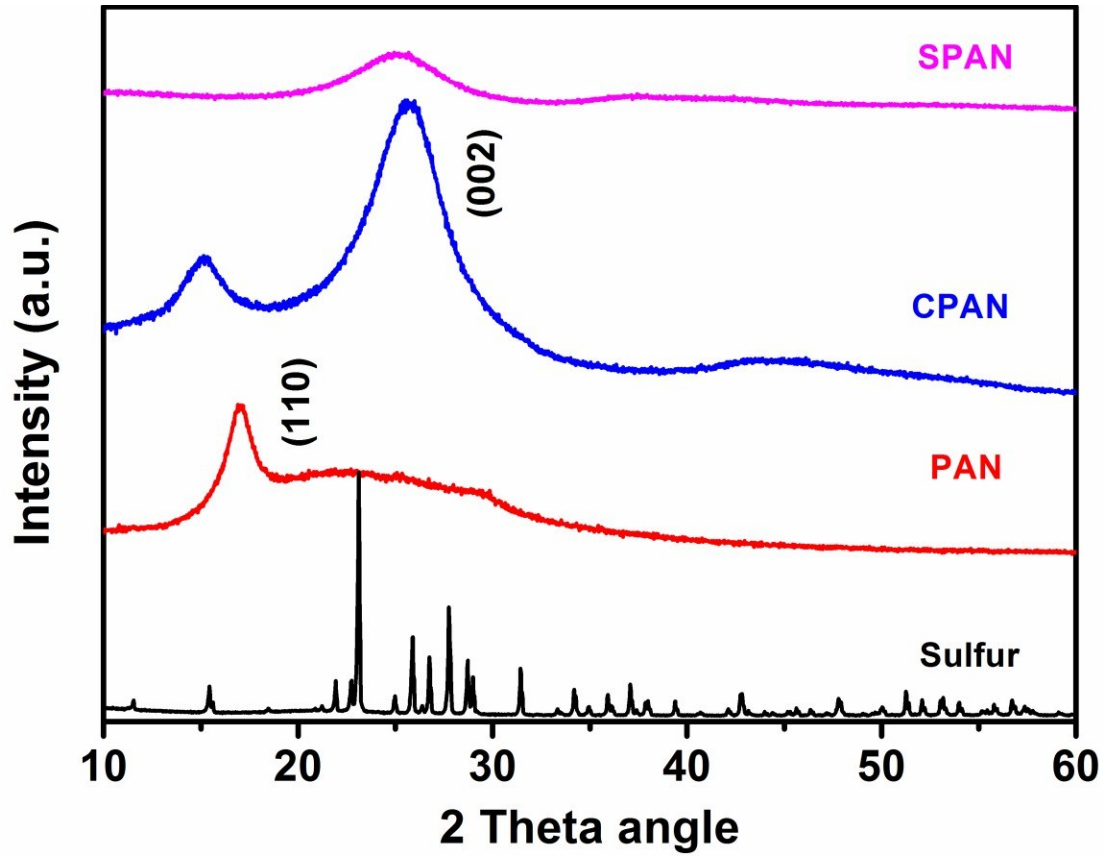

Figure S2. XRD patterns of SPAN, CPAN, PAN, and elemental Sulfur.

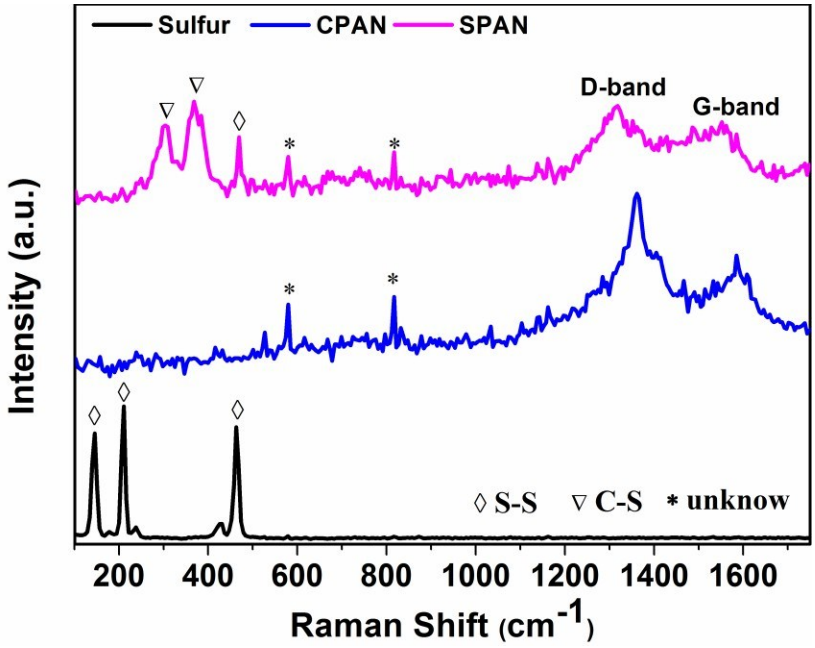

Figure S3. Raman spectra of SPAN, CPAN, and Sulfur.

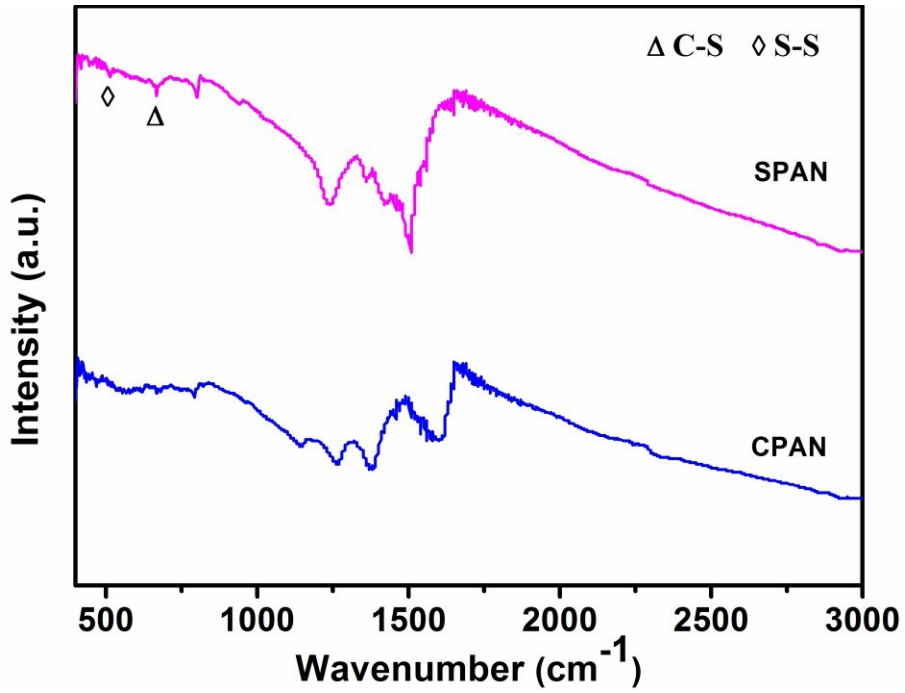

Figure S4. FT-IR spectra of SPAN and CPAN

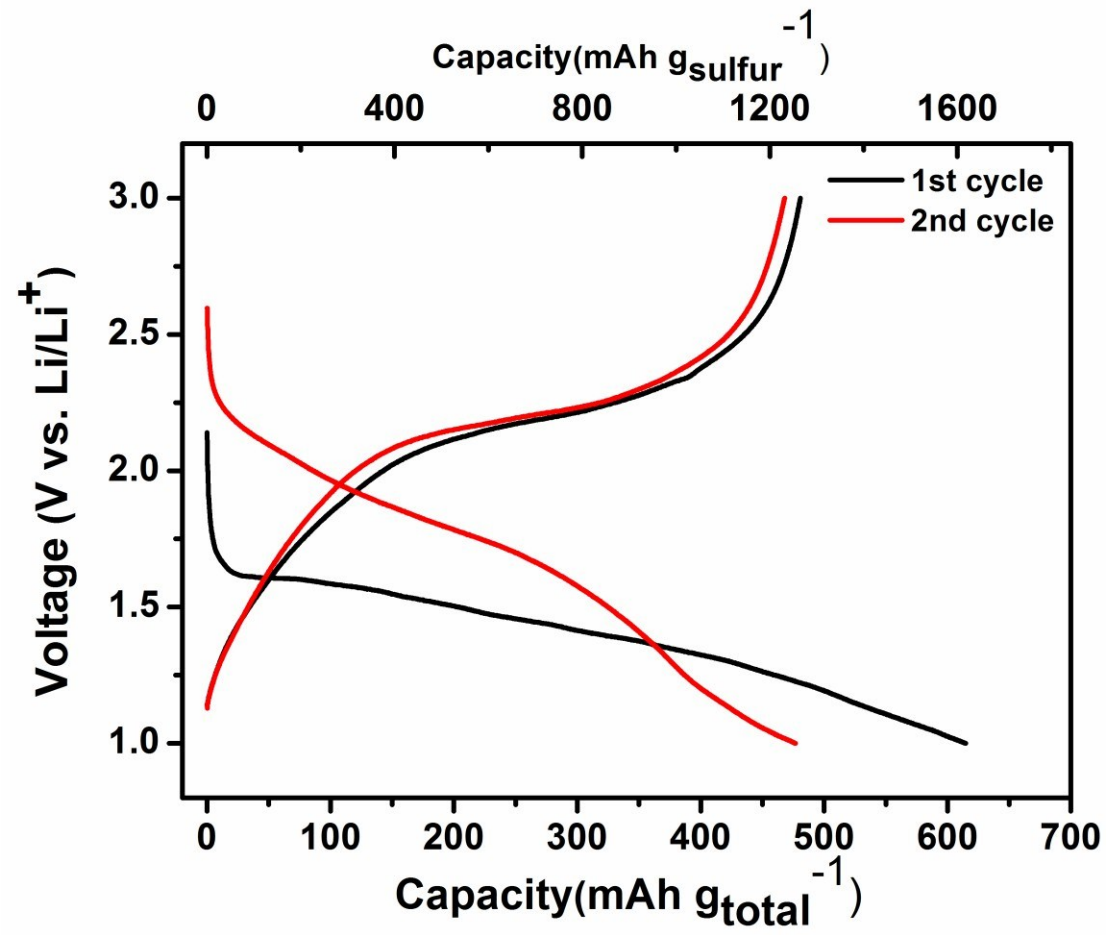

Figure S5. Electrochemical discharge and charge curves of SPAN toward Li at 1 C for the first two cycles in the potential range of 1–3 V vs Li/Li^+.

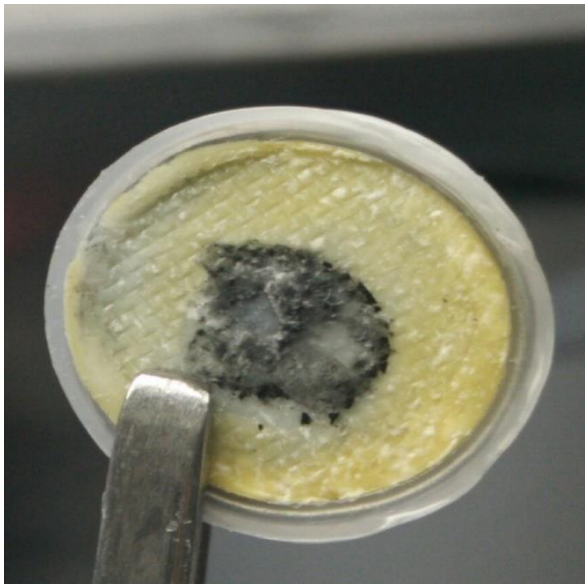

Figure S6. Digital image of glass-fiber separator inside a K-SPAN coin cell after 500 cycles, taken in a glovebox, showing the separator turns yellowish after cycling, possibly due to the decomposition of electrolyte.

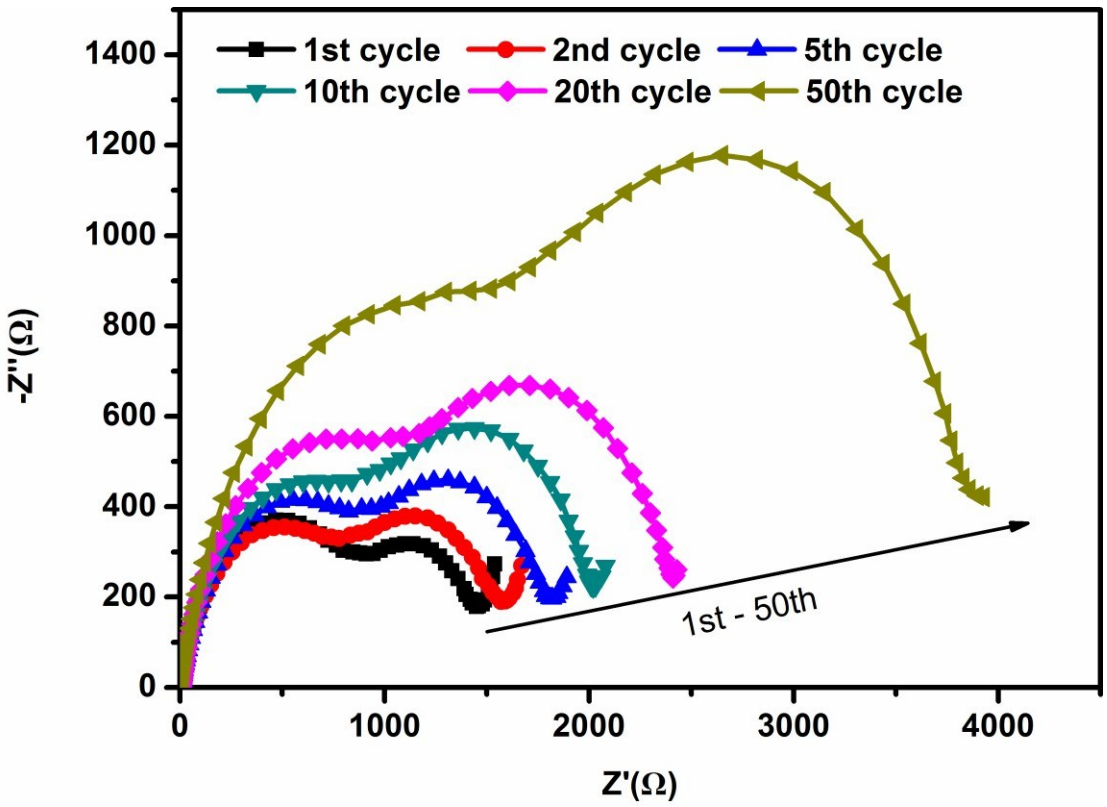

Figure S7. The Nyquist plots of the fully charged SPAN after cycling at 1 C for different times.

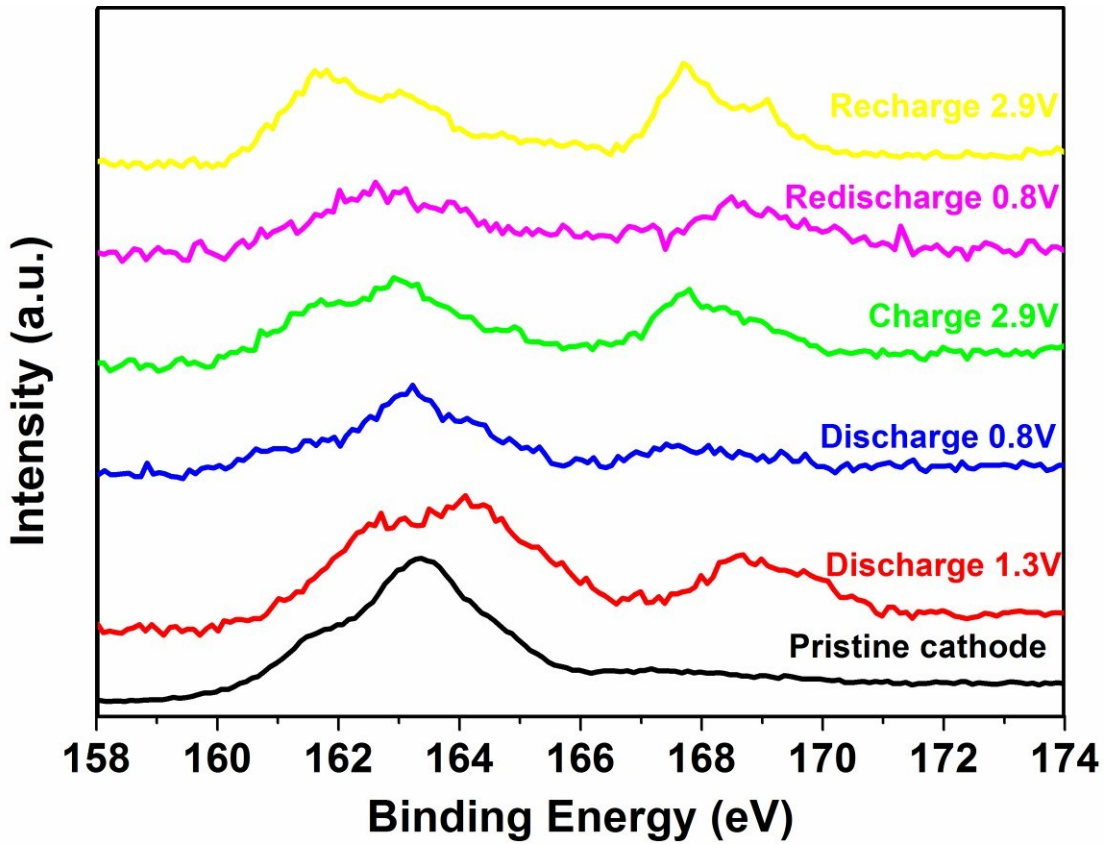

Figure S8. Ex-situ S 2p XPS spectra of SPAN during the first two cycles.

Table S1. Electrochemical performances of positive electrode materials for K-ion and K- batteries.

Material	Voltage Range(V)	Capacity (mAh/g) at Current density (A/g)	Initial capacity (mAh/g)	2nd capacity (mAh/g)	Highest capacity (mAh/g)	Cycle performance	Stable CE	Longest cycle number	Ref.
SPAN	0.8 - 2.9	265.5, 0.025 228, 0.075 200, 0.125 160, 0.25 111, 0.5 83.7, 0.75	270.2	270.5	275.2	149 mAh/g after 100 cycle at 0.125 A/g	~100%	100 cycle	This work
$KVPO_4F$	2.0 - 4.8	~76, 0.013 ~75, 0.026 ~73, 0.0665 ~72, 0.133 ~71, 0.266 ~70, 0.399 ~67, 0.665	~68	~70	~72	~70 mAh/g after 50 cycle at 0.013 A/g	~90%	50 cycle	2
$KVOPO_4$	2.0-4.8	~70, 0.0133-0.226 ~69, 0.399 ~67, 0.532 ~66, 0.665	~65	~68	~73	~70 mAh/g after 50 cycle at 0.013 A/g	~90%	50 cycle	2
$KTi_2(PO_4)_3$	1.2 -2.8	~80, 0.064 ~78, 0.128 ~73, 0.256 ~65, 0.64	~75.6	~72.6	~90	83 mAh/g after 100 cycle at 0.064 A/g	~100%	100 cycle	3

$K_3V_2(PO_4)_3$	2.5 - 4.3	54, 0.02 45, 0.05 30, 0.1 25, 0.2	54	53	54	52 mAh/g after 100 cycle at 0.02 A/g	~100%	100 cycle	4
$K_{0.67}Ni_{0.17}Co_{0.17}Mn_{0.66}O_2$	2.0 - 4.3	76.5, 0.02 70.2, 0.04 65.6, 0.06 58, 0.08 49, 0.1	76.5	76	76.5	66.8 mAh/g after 100 cycle at 0.02 A/g	~100%	100 cycle	5
KPBNP	2.0 - 4.0	76, 0.05 65, 0.1 56.1, 0.2 46.1, 0.3 36, 0.4	76.7	74.5	76.7	73.2 mAh/g after 100 cycle at 0.05 A/g	~90%	150 cycle	6
PTCDA	1.5 -3.5	117, 0.05 92, 0.1 88, 0.2 73, 0.5	117		117	90 mAh/g after 200 cycle at 0.05 A/g	~100%	200 cycle	7
PAQS	1.5 -3.4	198, 0.02	211	198	211	142.5 mAh/g after 50 cycle at 0.02 A/g	~100%	50 cycle	8
NI-KMHCF	2.5 -4.6	/	~86	~95	~110	~100 mAh/g after 100 cycle at 0.156 A/g	~100%	100 cycle	9
PANI@CMK-3/S	1.2 - 2.4	~500, 0.05	523.5 $mAh/(g_{sulfur}^{-1})$	490 $mAh/(g_{sulfur}^{-1})$	523.5 $mAh/(g_{sulfur}^{-1})$	329.3 $mAh/(g_{sulfur}^{-1})$ after 50 cycle at 0.05 A/g	~100%	50 cycle	10
Sulfur (150℃)	12 - 3.0	~400, 0.33mA /cm^2; ~320, 1.32; ~300, 2.31; ~285, 3.3; 260, 9.9	~280		~310	~300 mAh/g after 100 cycle at 2.31mA /cm^2	~100%	1000 cycle	11

References:

1. J. L. Wang, J. Yang, J. Y. Xie and N. X. Xu, *Adv. Mater.*, 2002, **14**, 963.
2. K. Chihara, A. Katogi, K. Kubota and S. Komaba, *Chem. Commun.*, 2017, **53**, 5208-5211.
3. J. Han, Y. Niu, S. J. Bao, Y. N. Yu, S. Y. Lu and M. Xu, *Chem. Commun.*, 2016, **52**, 11661-11664.
4. J. Han, G.-N. Li, F. Liu, M. Wang, Y. Zhang, L. Hu, C. Dai and M. Xu, *Chem. Commun.*, 2017, **53**, 1805-1808.
5. C. Liu, S. Luo, H. Huang, Z. Wang, A. Hao, Y. Zhai and Z. Wang, *Electrochem. Commun.*, 2017, **82**, 150-154.
6. C. Zhang, Y. Xu, M. Zhou, L. Liang, H. Dong, M. Wu, Y. Yang and Y. Lei, *Adv. Funct. Mater.*, 2017, **27**, 1604307.
7. Y. Chen, W. Luo, M. Carter, L. Zhou, J. Dai, K. Fu, S. Lacey, T. Li, J. Wan, X. Han, Y. Bao and L. Hu, *Nano Energy*, 2015, **18**, 205-211.
8. Z. Jian, Y. Liang, I. A. Rodríguez-Pérez, Y. Yao and X. Ji, *Electrochem. Commun.*, 2016, **71**, 5-8.
9. L. Xue, Y. Li, H. Gao, W. Zhou, X. Lu, W. Kaveevivitchai, A. Manthiram and J. B. Goodenough, *J. Am. Chem. Soc.*, 2017, **139**, 2164-2167.
10. Q. Zhao, Y. X. Hu, K. Zhang and J. Chen, *Inorg. Chem.*, 2014, **53**, 9000-9005.
11. X. Lu, M. E. Bowden, V. L. Sprenkle and J. Liu, *Adv. Mater.*, 2015, **27**, 5915-5922.